Thin ZIF-8 Nanosheets Synthesized in Hydrophilic TRAPs

Koki Sasaki, Tsuyoshi Okue, Yasuhiro Shu, Koji Miyake, Yoshiaki Uchida* and Norikazu Nishiyama

Graduate School of Engineering Science, Osaka University, 1-3 Machikaneyama-cho, Toyonaka, Osaka 560-8531, Japan

Supporting Information

Table of Contents

Characterization methods

X-ray Diffraction (XRD) Measurements

The crystal structures were estimated from XRD patterns collected using a PANalytical X'Pert PRO diffractometer with Cu Kα radiation, operated at 45 kV and 40 mA. The scan range was from 30º to 90º (2θ) at 0.10º/s. The full width at half maximum was calculated using X'Pert Data Viewer.

Atomic Force Microscopy (AFM)

AFM images were obtained using a Veeco Instruments MMAFM-2. The samples were deposited on freshly exfoliated mica sheets as substrates. We measure 30 samples and calculated the average and standard deviation of the size and thickness, respectively.

Transmission Electron Microscope (TEM)

TEM images were obtained using a Hitachi H-800 at 200 kV.

Dynamic Light Scattering (DLS)

The distributions of ZIF-8 NSs were measured by DLS using ELSZ-2000 (Otsuka Electronics Co., Ltd.) at 25°C.

Nitrogen adsorption

Nitrogen adsorption isotherm was measured by a BELSORPmax (MicrotracBEL) at 77 K.

X-ray photoelectron spectroscopy (XPS)

X-ray photoelectron spectroscopy (XPS) spectrum on C 1s and N 1s were obtained in a VG-Microtech Multilab 3000 spectrometer with an Al Kα radiation (1253.6 eV) as the energy sour.

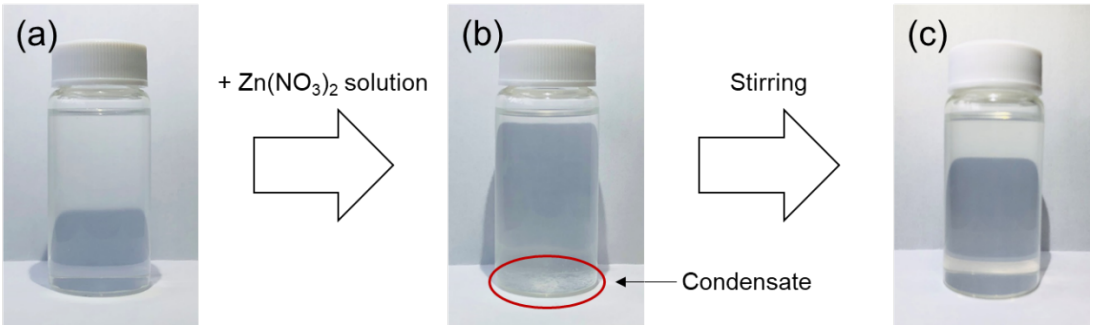

Fig. S1 Addition of the aqueous $Zn(NO_3)_2$ solution to the decane solution of hydrophilic TRAPs. (a) Before adding the aqueous $Zn(NO_3)_2$ solution, the decane solution is clear. (b) The mixture becomes turbid once immediately after adding $Zn(NO_3)_2$. (c) After stirring, the mixture becomes clear again.

Table S1 XRD peak positions and full width at half maximum for ZIF-8 NSs and conventional ZIF-8 crystals.

Peak (2θ)	Full width at half maximum (°)	
	Nanosheets	Conventional
7.4	0.355	0.291
10.4	0.356	0.286
12.8	0.371	0.297
14.7	0.388	0.303
16.5	0.384	0.308
18.1	0.397	0.316
19.6	0.380	0.315
22.3	0.374	0.312
24.6	0.451	0.311
25.7	0.404	0.316
26.8	0.435	0.324
29.8	0.427	0.317
30.7	0.409	0.334
31.7	0.388	0.326
32.5	0.404	0.326

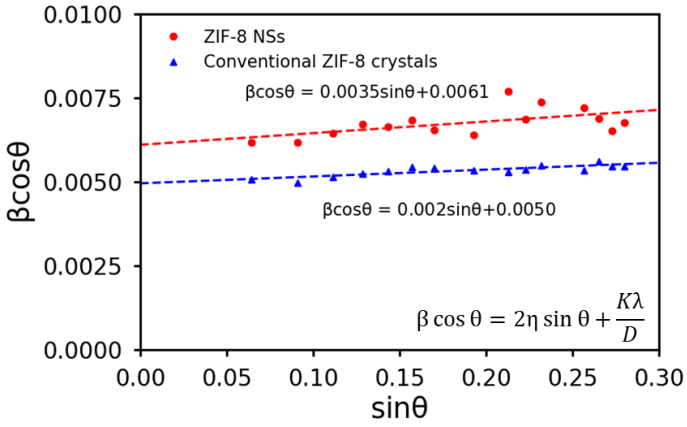

Fig. S2 Williamson-Hall plots of the ZIF-8 NSs and conventional ZIF-8 crystals. In the equations, β is full width at half maximum, η is internal strain, *K* is Scherrer constant, λ is the X-ray wavelength, and *D* is crystallite size. The Scherrer constant used was 0.94 for cubic symmetry. The estimated *D* for the ZIF-8 NSs and conventional ZIF-8 crystals are 24 nm and 29 nm, respectively.

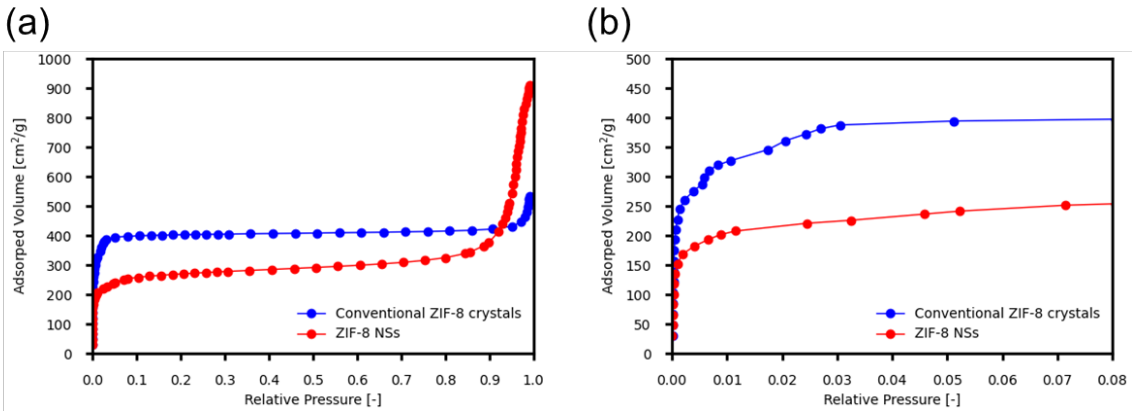

Fig. S3 Nitrogen adsorption isotherms of ZIF-8 NSs and conventional ZIF-8 crystals. Relative pressure ranges from 0 to (a) 1, and (b) 0.08.

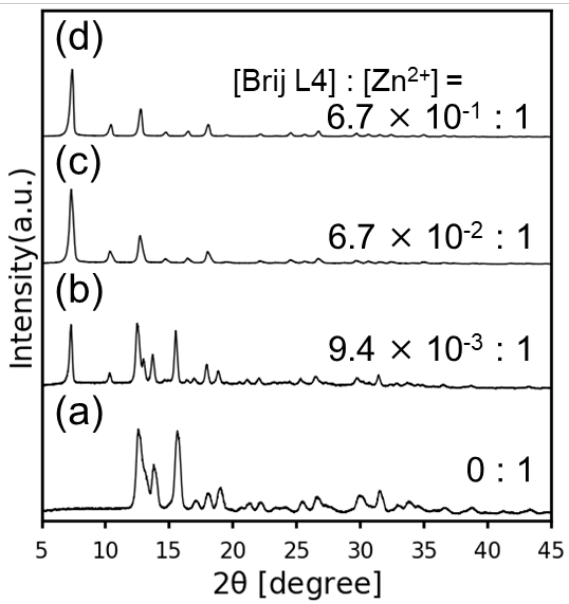

Fig. S4 XRD patterns of zinc 2-methylimidazolate synthesized with various concentration of Brij L4. The ratios of [Brij L4]/[Zn^{2+}] are (a) 0, (b) 9.4×10^{-3}, (c) 6.7×10^{-2}, and (d) 6.7×10^{-1}.

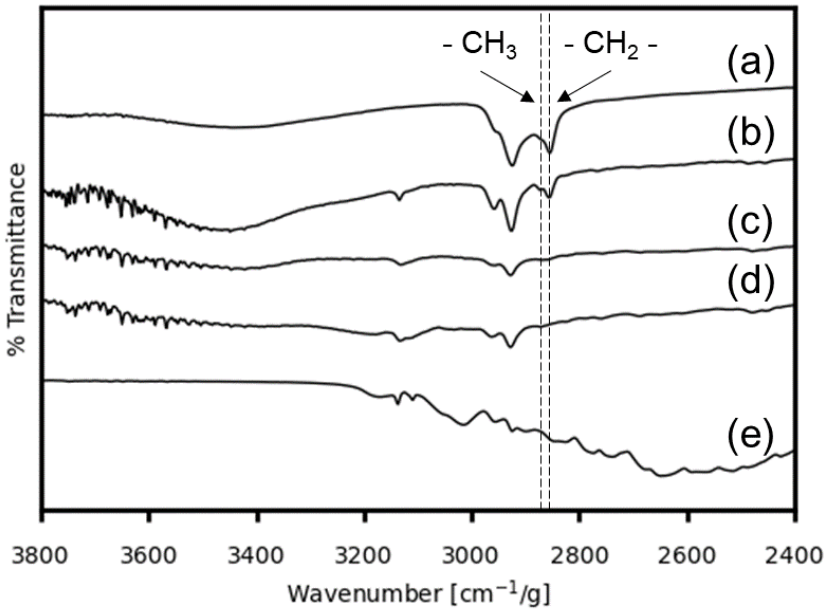

Fig. S5 FT-IR spectra of (a) Brij L4 and (b) ZIF-8 NSs, zinc 2-methylimidazolate synthesized (c) with Brij L4 and (d) without Brij L4, and (e) 2-methylimidazole.

Fig. S6 Polarized photograph of a hyperswollen lyotropic lamellar phase of decane solution of Brij L4 (1.8×10^{-1} M), water (1.0 M), ammonium hydroxide (1.2×10^{-2} M), 2-mim (2.8×10^{-3} M), $Zn(NO_3)_2$ (1.2×10^{-3} M), and $Co(NO_3)_2$ (6.1×10^{-5} M).

Table S2 XRD peak positions and full width at half maximum for Co-ZIF-8 NSs and conventional Co-ZIF-8 crystals.

Peak (2θ)	Full width at half maximum (°)	
	Nanosheets	Conventional
7.2	0.330	0.265
10.2	0.335	0.274
12.6	0.335	0.282
14.6	0.327	0.284
16.3	0.331	0.283
17.9	0.356	0.298
19.4	0.282	0.293
22.0	0.366	0.293
24.4	0.314	0.305
25.5	0.330	0.318
26.5	0.346	0.300
29.5	0.404	0.293
30.5	0.348	0.335
31.4	0.325	0.286
32.3	0.392	0.307

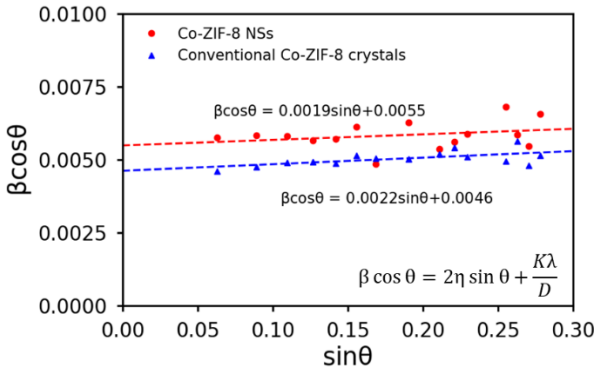

Fig. S7 Williamson-Hall plots of Co-ZIF-8 NSs and conventional Co-ZIF-8 crystals. In the equations, β is full width at half maximum, η is internal strain, *K* is Scherrer constant, λ is the X-ray wavelength, and *D* is crystallite size. The Scherrer constant used was 0.94 for cubic symmetry. The estimated *D* for Co-ZIF-8 NSs and conventional Co-ZIF-8 crystals are 26 nm and 31 nm, respectively.

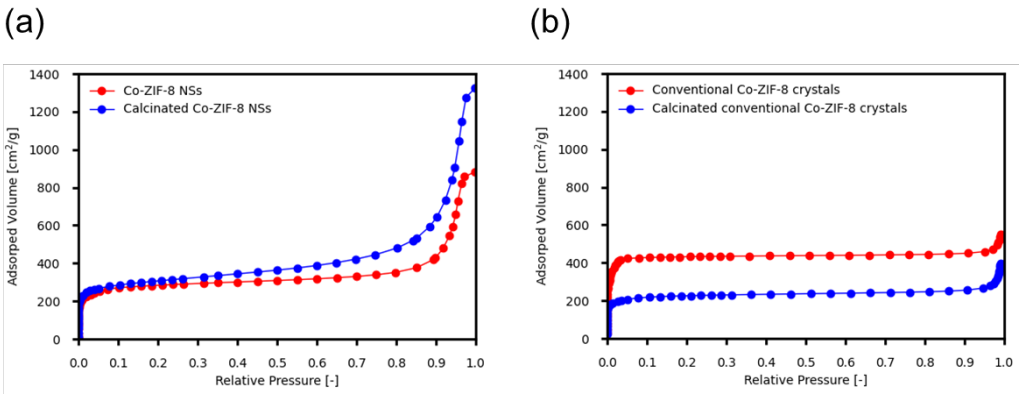

Fig. S8 Nitrogen adsorption isotherms of (a) Co-ZIF-8 NSs and (b) conventional Co-ZIF-8 crystals before and after calcinated Co-ZIF-8 NSs and conventional Co-ZIF-8 crystals.

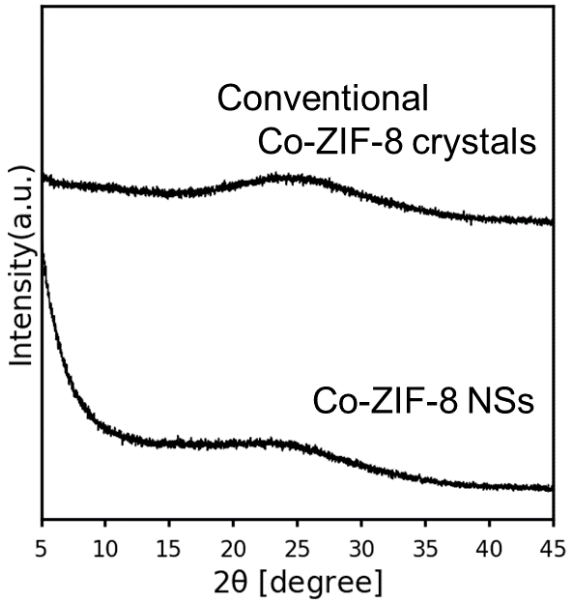

Fig. S9 X-ray diffraction patterns of the Co-ZIF-8 NSs, and conventional Co-ZIF-8 crystals after calcination.

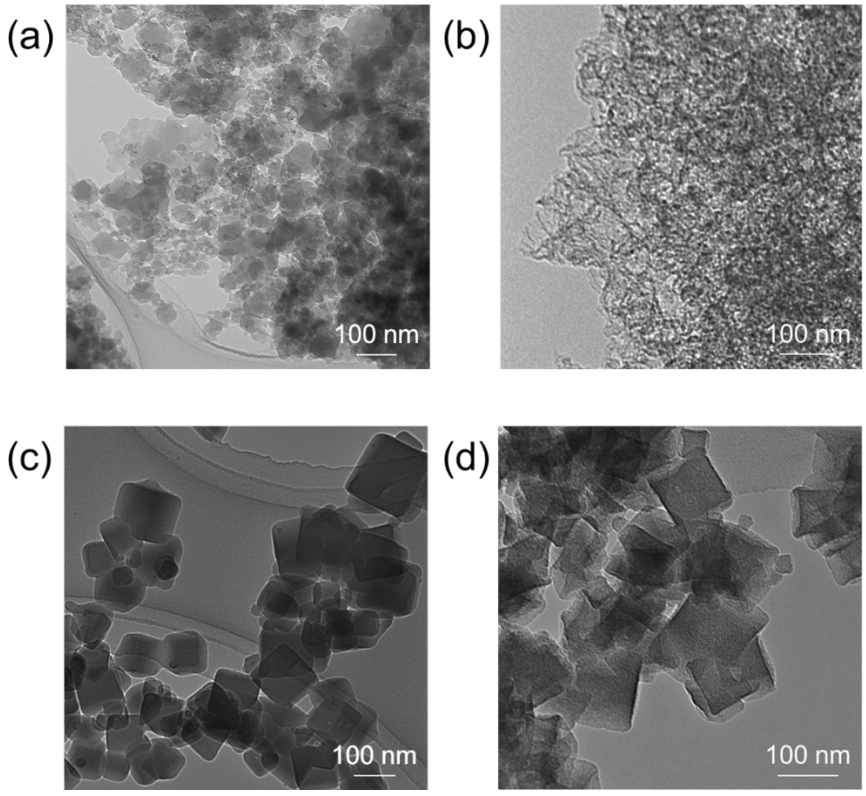

Fig. S10 TEM photographs of Co-ZIF-8 NSs (a) before and (b) after calcination, and of conventional Co-ZIF-8 crystals (c) before and (d) after calcination.

Table S3 Total surface areas and pore volumes of Co-ZIF-8 NSs and conventional Co-ZIF-8 crystals measured by nitrogen adsorption isotherms.

Sample	S_{total} (m^2/g)	V_{micro} (< 2 nm) (cm^3/g)	V_{meso} (2 - 50 nm) (cm^3/g)	V_{macro} (> 50 nm) (cm^3/g)	V_{total} (cm^3/g)
Conventional	860	0.35 (57 %)	0.09 (15 %)	0.17 (28 %)	0.6
Nanosheets	1130	0.31 (15 %)	1.20 (59 %)	0.51 (25 %)	2.02

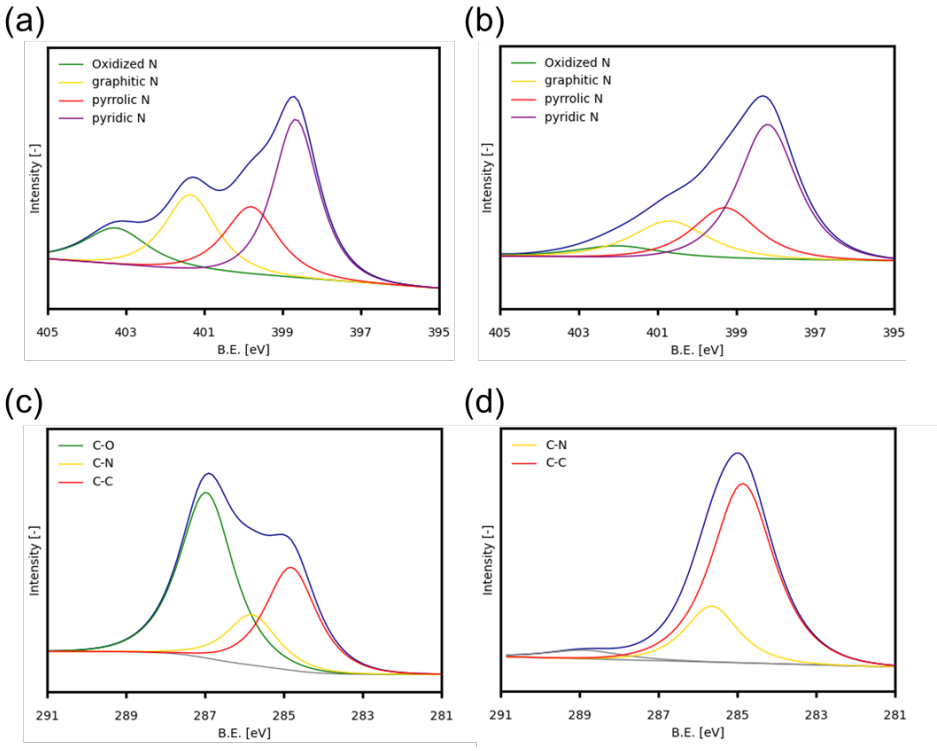

Fig. S11 XPS spectra of N 1s of (a) calcinated Co-ZIF-8 NSs and of (b) calcinated conventional Co-ZIF-8 crystals, and C 1s of (c) calcinated Co-ZIF-8 NSs and of (d) calcinated conventional Co-ZIF-8 crystals.